

Applying High Speed De-Compensated VFA's: Hitting Performance Targets while Tuning Phase Margin, Insight #10.

Michael Steffes, Sr. Applications Manager, July 2019

Most high-speed Voltage Feedback Amplifier (VFA) product developments have focused on the unity gain stable type, with far fewer offerings in decompensated VFAs. Those seem to come with more oscillation risk but can offer improved dynamic range vs quiescent power. Here, some typical applications particularly suited to a decompensated VFA solutions will be shown with phase margin improvement techniques where needed. A sampling of vendor solutions across different process technologies will show the range of available high speed decompensated VFAs.

What is a de-compensated VFA - and why would you use it?

Starting from a typical unity gain stable VFA, to get a decompensated version, IC designers would normally –

1. Increase the input stage transconductance – reducing the degeneration resistors - normally lowering the input spot noise voltage.
2. Decrease the dominant pole compensation capacitor just in front of the output stage buffer. With the same total supply current, this will normally increase the available slew rate along with increasing the Gain Bandwidth Product (GBP).

Using the same total quiescent current, a decompensated version will have a higher GBP, a higher slew rate, and lower input voltage noise. The initial intent for this type of device was simply to provide higher closed loop bandwidths when operated at higher gains. Using a few simple external design tricks, you can also use these to provide higher Loop Gain (LG) at lower frequencies – which is one path to lowering the harmonic distortion. Figure 1 shows the simplest higher gain application using the decompensated OPA838 bipolar device (Reference 1). This is using the R_f and R_g values from Table 1, Reference 1. Those values were developed solving for the R_f value that gives a total resistor noise power contribution at the output at 40% of the total and considering the added loop phase shift due the $R_f || R_g$ driving the input pin parasitic capacitance. Lower R values would reduce the total output noise but then start to add meaningfully to the total power consumption over just the 1mA quiescent current for the OPA838. The R_s at the V+ input is added to achieve bias current cancellation for this bipolar input device. That R_s does increase the total output noise and should be replaced by a 10ohm value if DC precision is not a concern.

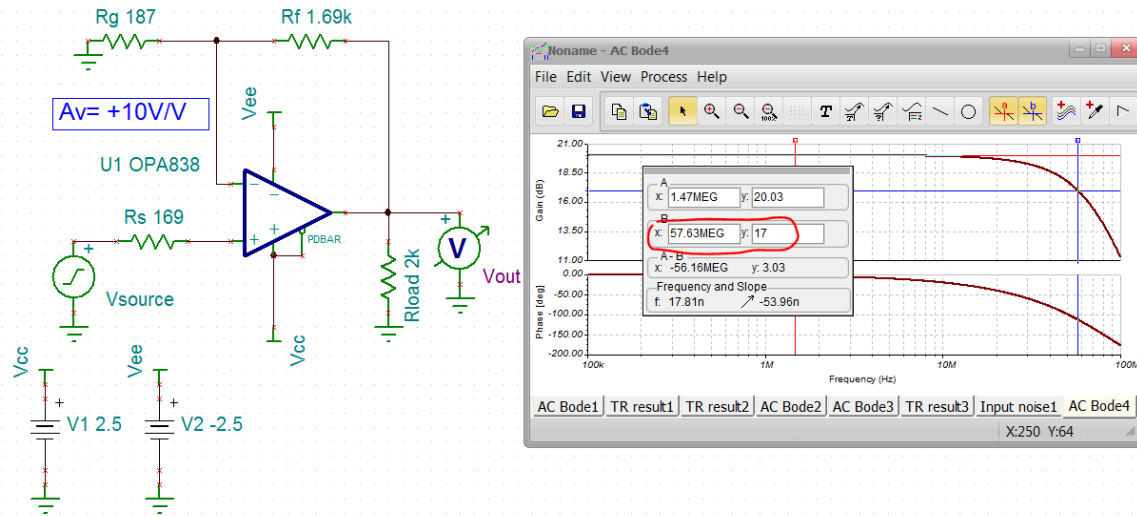


Figure 1. Non-inverting gain of 10V/V using the decompensated OPA838 and recommended R values.

Running a Loop Gain (LG) Phase Margin (PM) test in Figure 2 shows a $LG=0\text{ dB}$ at 28.5 MHz with 64 deg phase margin. This would suggest (Figure 4, Reference 2) a $1.56 \times 28.5\text{ MHz} = 44.5\text{ MHz}$ $F_{-3\text{ dB}}$ where the actual bandwidth shown in Figure 1 is 58 MHz . While the $LG=0\text{ dB}$ frequency closely matches the expected GBP of 300 MHz divided by the Noise Gain (NG) of 10, quite a lot more closed loop bandwidth is delivered due to the $PM < 90\text{ deg}$ effect. The added $F_{-3\text{ dB}}$ extension (over Fig. 4 Reference 2) is probably due to the $> 2^{\text{nd}}$ order A_{ol} model and the reactive open loop output impedance in the model. The feedback LG measurement point in Figure 2 reports phase margin directly with the polarity shown and includes the internal input impedance model elements (Reference 3) along with the R_s element on the $V+$ input.

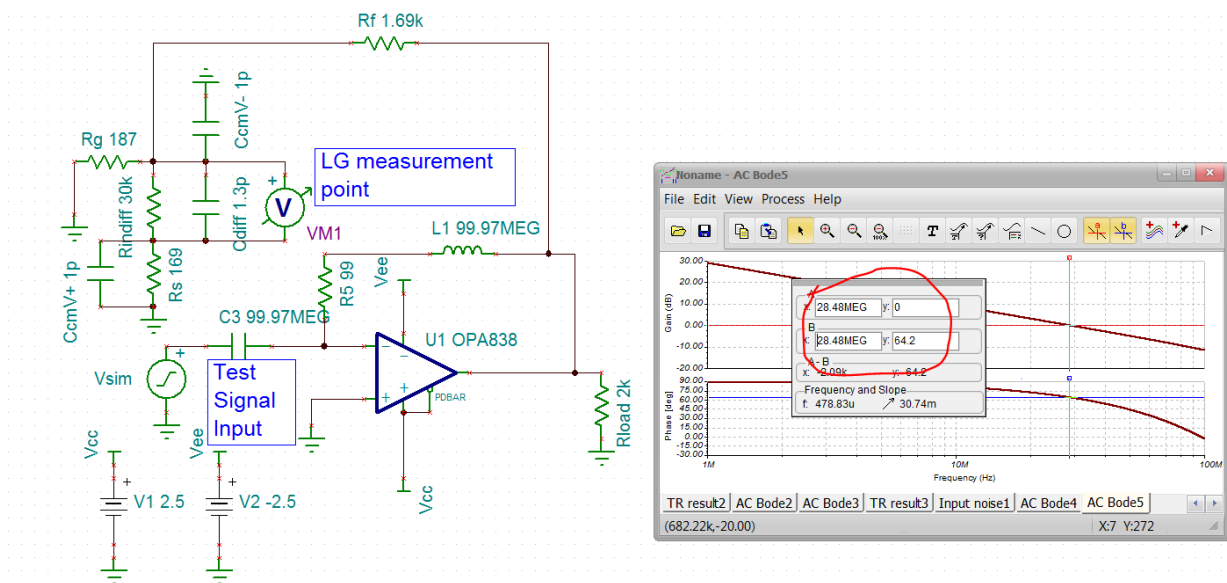


Figure 2. Gain of +10V/V Loop Gain simulation for phase margin.

Extending inverting operation to lower gains using decompensated VFAs

Moving beyond the simple non-inverting application at higher gains, if the application can use an inverting configuration, a simple external compensation can be used to operate at any inverting gain (including attenuation) applying a de-compensated VFA. Legacy literature (Page 14, Reference 4) also suggests a lead/lag compensation across the input pins (a series RC) to operate at low gains. This works, but does introduce a response zero impairing frequency response flatness and settling time. This simpler two capacitor inverting compensation approach (Reference 5) actually remains 2nd order with no zeroes providing an easily tuned closed loop response. The earlier illustrations using this technique matched theory very well with non-RR output stages having low open loop output impedance. More recent RR output stages with highly reactive open loop output impedances in their models still work, but do not match the simpler analysis in Reference 5 as well.

The general analysis of Reference 5 was later simplified to a closed loop Butterworth target as shown in equations 4 -> 7 in the OPA847 datasheet (Reference 6). The two capacitors in Figure 4 (using the newer OPA838 - Reference 1) are shaping the Noise Gain (NG) up with frequency to achieve a Loop Gain (LG) =0dB crossover at a high enough NG to maintain stability for this de-compensated device. This does reduce the closed loop bandwidth but retains the full rated slew rate and a low input noise at frequencies below the NG zero frequency. The two key Noise Gains (NG) are the low frequency NG₁ and then the higher frequency NG₂.

$$\boxed{NG_1 = 1 + \frac{R_f}{R_g}} \quad \text{Eq. 1}$$

$$\boxed{NG_2 = 1 + \frac{C_s}{C_f}} \quad \text{Eq. 2}$$

To solve for a nominally Butterworth closed loop response, use Equation 3 to get the Z_o – this is physically the projection of rising portion of the NG in a Bode plot projected back to its 0dB intersection.

$$\boxed{Z_o = \frac{GBP}{NG_1^2} \left(1 - \frac{NG_1}{NG_2} - \sqrt{1 - 2 \frac{NG_1}{NG_2}} \right)} \quad \text{Eq. 3}$$

The actual NG zero frequency will occur at NG₁*Z_o.

With Z_o resolved, the required C_f will be given by Equation 4

$$\boxed{C_f = \frac{1}{2\pi R_f Z_o NG_2}} \quad \text{Eq. 4}$$

And finally, the required C_s on the inverting node to ground is solved using Equation 5

$$C_s = (NG_2 - 1)C_f$$

Eq. 5

For devices that do not have a highly reactive open loop output impedance, the resulting closed loop F_{-3dB} bandwidth is approximately given by Equation 6

$$F_{-3dB} \approx \sqrt{GBP * Z_o}$$

Eq. 6

A graphical interpretation of what is going on with this inverting compensation is shown in Figure 3 (Figure 2, Reference 5). Here, only the dominant op amp A_{ol} pole is shown. Any actual decompensated op amp will have higher frequency poles that will move the true $A_{ol} = 0dB$ crossover away from the ideal projected frequency. However, the $LG=0dB$ frequency is being pulled way back by the compensation to occur in a region easily modeled as only a dominant pole model.

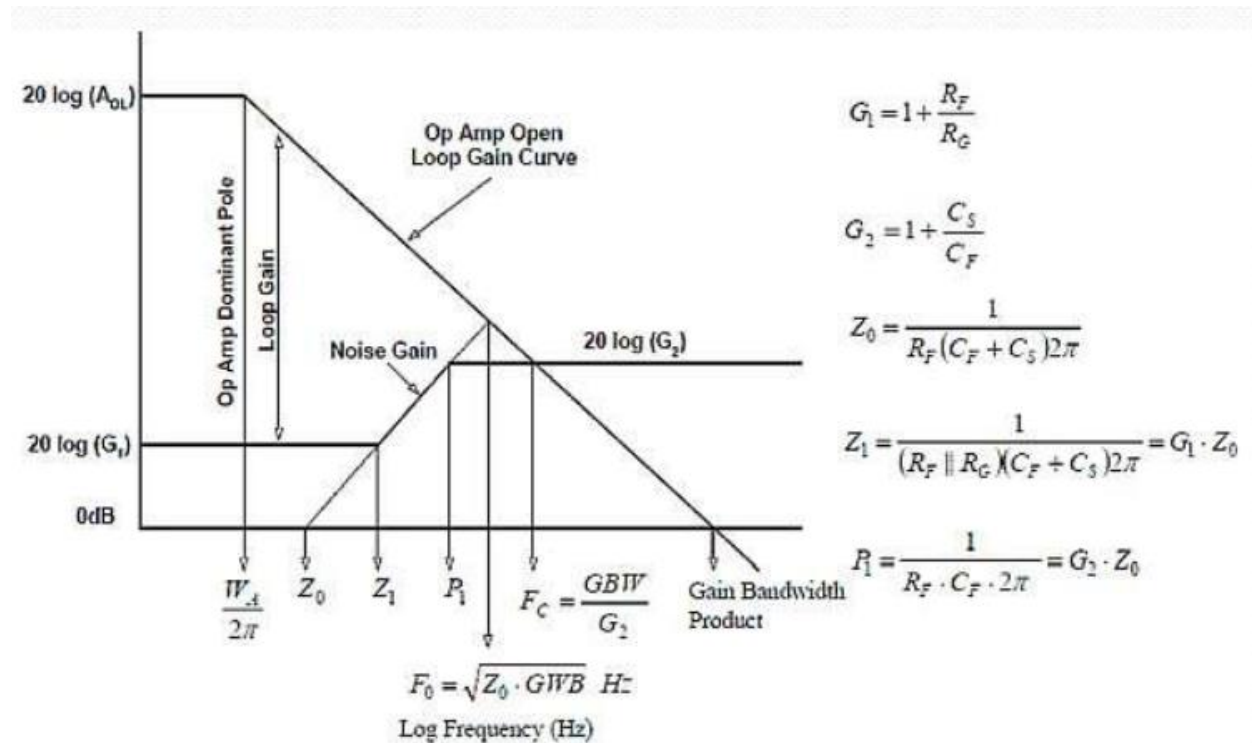


Figure 3. Bode plot of op amp A_{ol} and the NG for the inverting compensation approach.

To step through an example design, start by picking an R_f that is relatively low to hold its noise contribution down. Select

- $R_f = 499\Omega$.
- Set the target gain to $-2V/V$ - then $R_G = 249\Omega$.
- This gives us a low frequency $NG_1 = 3V/V$.

- d. Select a target high frequency $NG_2 > \text{min stable gain of } 7V/V \text{ at } 10V/V$.
- e. Using the 300MHz GBP of the OPA838, use Equation 3 to get $Z_0 = 2.25\text{MHz}$.
- f. Then the Z_1 in Figure 3 will be $3 * 2.25\text{MHz} = 6.75\text{MHz}$. Below this frequency the LG is increased by the compensation to deliver lower harmonic distortion.
- g. Using Z_0 and Equation 4, set the feedback $C_f = 14\text{pF}$.
- h. Then using Equation 5, set the capacitor to ground on the inverting input to 127pF which is reduced by the internal 2pF ($C_{\text{diff}} + C_{\text{cm}}$) to $C_s = 125\text{pF}$.
- i. The approximate closed loop bandwidth is estimated by Equation 6 to be 26MHz .

Figure 4 shows the resulting closed loop responses for different external conditions. Clearly, the two compensation capacitors are required to operate at this lower than minimum stable gain condition. The response shape with the compensation capacitors is peaking more than expected with extended bandwidth. Isolating the effect of the open loop output impedance by using a dependent source (fig. 7, Reference 2) shows a much better Butterworth fit with a $33\text{MHz } F_{-3\text{dB}}$ nearly matching the expected 26MHz value.

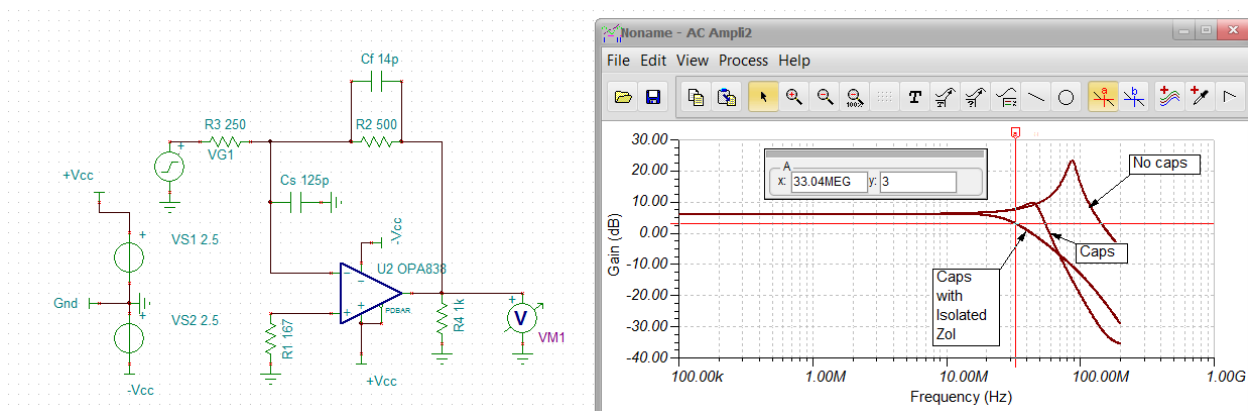


Figure 4. Gain of $-2V/V$ inverting compensation using the OPA838.

While the basic idea of this inverting compensation still works with the RR output OPA838, the added poles around the loop due to its reactive open loop output impedance move the resulting closed loop shape off the earlier theory. Decompensated wideband op amps with lower open loop output impedance using a non-RR output design (like the OPA818, Reference 7) will fit the expected shape much better. Figure 5 shows the Loop Gain (LG) simulation of Figure 4. The meter is rotated to report Phase Margin (PM) directly. This 21deg phase margin is much lower than the closed loop peaking in Figure 4 might suggest. Note the full input impedance model and the bias current cancellation resistor on the $V+$ input to ground are included here to develop the differential feedback voltage. This lower than expected PM, and lower peaking than expected for that PM in the response shape, are due to the OPA838's reactive open loop output impedance model (Z_{ol}). To move closer to theory in the next two examples, a non-RR output decomp JFET device (OPA818) with much lower Z_{ol} (Figure 5, Reference 7) will be used.

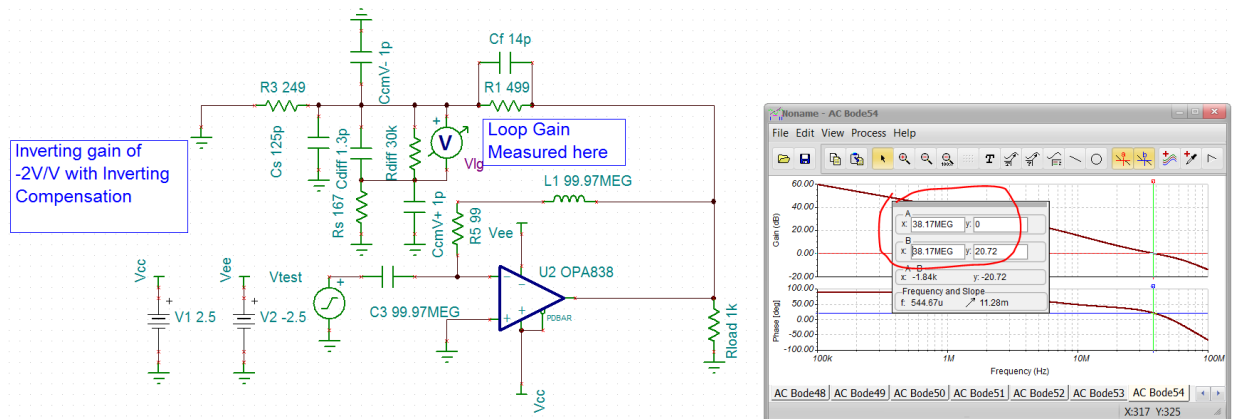


Figure 5. Inverting Compensation LG simulation using the OPA838

Using a Decompensated VFA in a Multiple Feedback (MFB) Active Filter

Another very common VFA application would be in an MFB (or Rauch) active filter. Legacy literature constrains these solutions to unity gain stable VFA devices since the direct feedback capacitor required by the topology shapes the NG to unity gain at higher frequencies. However, a direct extension of the inverting compensation technique described above will allow decompensated devices to be applied to MFB solutions (Reference 8). Expanding the solution universe to decompensated devices will allow much higher slew rate devices giving higher full power bandwidth and lower harmonic distortion. Use the 2.8GHz Gain Bandwidth Product (GBP) OPA818 to implement a 2nd order MFB design delivering –

1. Inverting gain of -5V/V
2. 5MHz F_{-3dB}
3. Butterworth response ($Q=0.707$)

The RC solution of Figure 6 is using a reduced noise and NG peaking flow (Reference 8) to get the filter RC values. The required added step is to target a higher frequency noise gain using the filter feedback C_2 and an added C_t to ground on the inverting summing junction. Targeting a capacitor divider NG of 10V/V for this minimum stable gain of 7V/V device gave the added 120pF to ground on the op amp's inverting node in Figure 6. This C_t capacitor can be included in the 3rd order transfer function coefficient polynomials for a GBP adjusted RC solution without increasing beyond 3rd order (Reference 9). Adding C_t will effectively reduce the available GBP by that higher frequency NG value - in this case reducing the available GBP to 280MHz for the MFB RC solutions. Some legacy MFB solution flows show a very high required GBP for this design point (1.77GHz from the TI active filter designer, Reference 10). However, accounting for the equivalent GBP in this design gave the reasonably accurate solution of Figure 6. These RC values are both adjusted for GBP (including the effect of C_t) and selected for the best fit E96 resistor and E24 capacitor values.

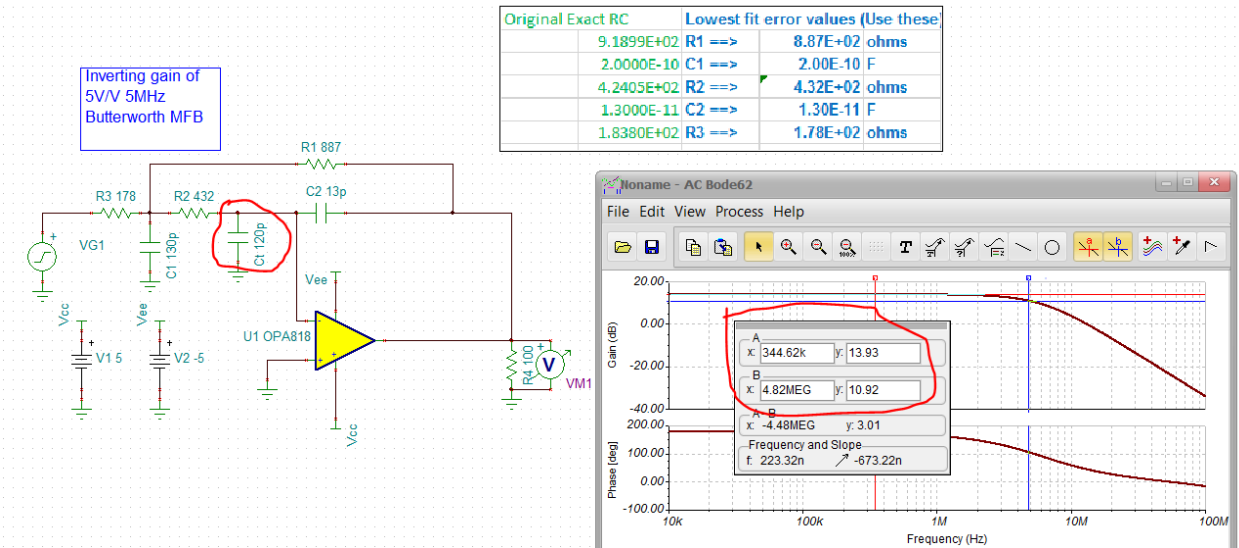


Figure 6. Inverting MFB design using the de-compensated OPA818.

Another important indicator of both active filter design margin and stability come from the LG simulation of Figure 7. This is showing a very good 31dB of LG at the filter $F_o = 5\text{MHz}$. Then, at the $\text{LG}=0\text{dB}$ frequency of 235MHz we also see a very good 55degrees phase margin. Removing that C_t capacitor moves the $\text{LG}=0\text{dB}$ crossover out to 956MHz with only 15degrees phase margin.

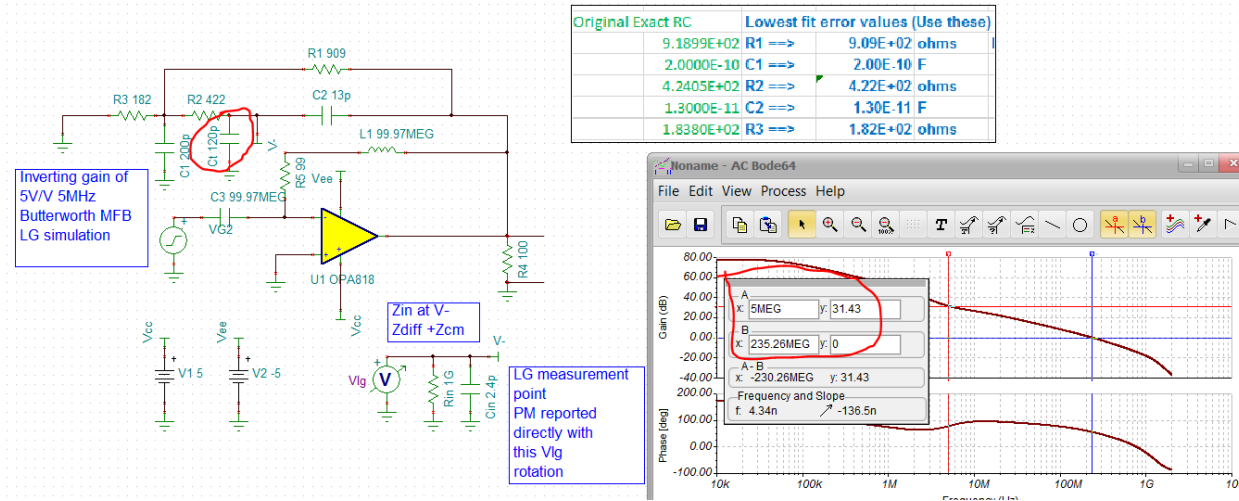


Figure 7. MFB filter LG simulation with C_t NG shaping capacitor.

This application of a decompensated VFA is of course peaking the output noise to get stability. Figure 8 shows the output spot noise with and without C_t in the design. The stable design will have an increased integrated noise to get that stability. The first peak in the output noise is the filter noise gain peak while the 2nd is the $\text{LG}=0\text{dB}$ crossover peak. A post RC filter can be used to reduce this higher integrated noise. Removing C_t definitely reduces the output spot noise but that sharp peak around 1GHz is typical of very low phase margin designs.

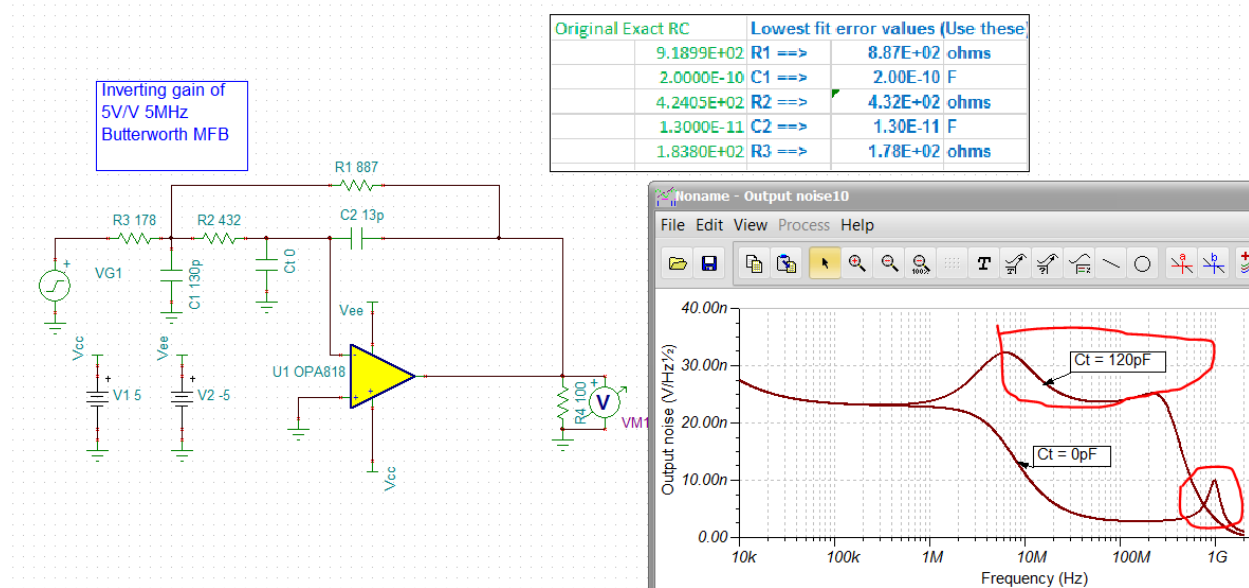


Figure 8. Output spot noise with and without C_t in the MFB filter design.

Essentially extending the inverting compensation approach to this active filter design easily allows decompensated VFAs to be applied to these MFB filter requirements. This can vastly extend the available full power bandwidth using the intrinsically higher slew rates available from decompensated devices. If possible, the full design flow should consider a simple post RC filter to reduce the more peaked output spot noise intrinsic to this approach. It does not appear at this time that any of the vendor online MFB design tools will apply a decompensated VFA to solutions. To force a solution, use a unity gain stable device, to be later replaced by a decompensated device with this added C_t targeting a high frequency noise gain to be developed later, and divide that into the decompensated GBP to get the equivalent unity gain device GBP to target. Execute a design with a device near that target using a unity gain stable device, then replace it with the decompensated device with the added C_t element.

Applying Decompensated VFA's to Photodiode Transimpedance Applications

Probably the most ubiquitous application of decompensated VFA's comes in the transimpedance application. The simplest form of this is just the detector capacitance, a feedback resistor that sets the gain, and (most importantly) a feedback capacitor that sets the Q of the closed loop response. The Bode plot for the loop gain is very similar to Figure 3 except the DC NG is 0dB (see Figure 2, Reference 11). One common assumption is that the feedback C_f will eventually be chosen to deliver a closed loop maximally flat Butterworth response. With that assumption, Equation 7 (Equation 12, Reference 11) gives the required GBP dependent on the other terms in the design. Increasing the desired gain (R_f), bandwidth, and source C_s all act to increase the required GBP in the VFA to deliver a closed loop 2nd order maximally flat Butterworth response shape.

$$GBP = 2\pi * F_{-3dB}^2 * R_f C_s \quad \text{Eq. 7}$$

The next key is to decide if a bipolar input or JFET input device is preferable. That normally becomes an input referred equivalent spot current noise question. The simplified expression in Equation 8 (Equation

13, Reference 11) applies when there is a postfilter at a frequency less than the feedback pole frequency. Making that assumption allows a simpler integration of the rising portion of the spot output noise due to the noise gain zero formed by the feedback resistor and source capacitance (C_s). Equation 8 is delivering the equivalent flat input current spot noise that will integrate to the same total output noise power as the highly peaked actual output noise response.

What this means in practice is the target F_{-3dB} in the transimpedance stage should be slightly higher than desired. This is a good practice in any case to account for GBP variation in the op amp stage where an extrinsic postfilter will deliver a lower tolerance operating bandwidth and constrain the integrated noise.

$$i_{eq} = \sqrt{i_b^2 + \frac{4kT}{R_f} + \left(\frac{e_n}{R_f}\right)^2 + \frac{(e_n 2\pi F_{NPBW} C_s)^2}{3}}$$
 Eq. 8

The F_{NPBW} is the Noise Power BandWidth (NPBW) in Hertz of the postfilter which needs to be less than the feedback pole frequency for Eq. 8 to be accurate. It is often difficult to predict which decompensated VFA will give the lowest input referred current noise as different combinations of terms in Equation 8 can be dominant depending on source capacitance, the NPBW, the gain, and the op amp noise terms. This often it comes down to trying different physical op amp terms in Equation 8. Normally, for transimpedance gains $> 100k\Omega$, a JFET or CMOS input device will be preferable.

Equation 7 can be used in a couple of ways to set the limits for a transimpedance design. Since increasing the feedback R_f uniformly reduces the input referred current noise as shown by equation 8, one common approach is to solve Equation 7 for the maximum R_f to satisfy the target F_{-3dB} with the source capacitance and available GBP in a candidate device as shown in Equation 9.

$$R_{f\max} = \frac{GBP}{2\pi * F_{-3dB}^2 * C_s}$$
 Eq. 9

Once we have this maximum gain to meet the intended bandwidth target, the last step is to solve for the required feedback C_f to hit that. Equation 10 shows an approximate solution that works very well where the Q relates to the desired or allowed frequency response peaking in the transimpedance stage.

$$C_f = \frac{1}{Q} \sqrt{\frac{C_s}{2\pi R_f GBP}}$$
 Eq. 10

Continuing with the OPA818 2.8GHz GBP JFET input device, target a final F_{-3dB} using a 2nd order passive Butterworth postfilter to 10MHz while targeting the transimpedance stage at 14MHz. Assume a 20pF diode capacitance and add the internal $C_{cm}=1.9pf + C_{diff} = 0.5pF$. Putting these numbers into Equation 9 yields –

$$R_{f\max} = 102k\Omega$$

And then solving for the required C_f to hit a $Q=0.707$ using Eq. 10 yields –

$$C_f = 0.16\text{pF}$$

Putting this into a TINA (Reference 12) simulation, along with an 11MHz 2nd order Butterworth RLC filter with only -1dB insertion loss (Reference 13), gives the design of Figure 9. Here, the response to the OPA818 output pin matches the 14MHz Butterworth target while combined with the 11MHz passive postfilter gives a nearly perfect 10MHz $F_{-3\text{dB}}$ to the output.

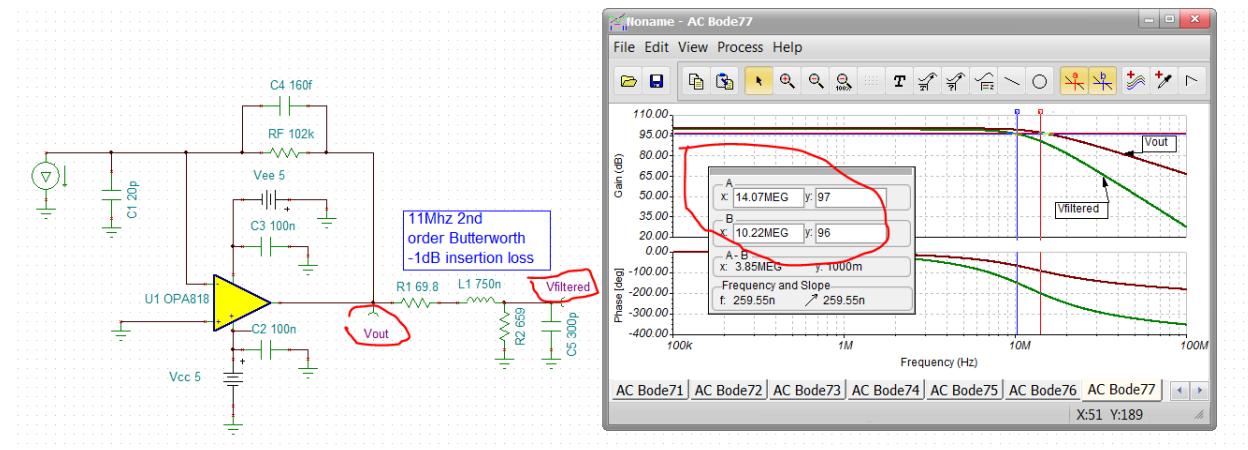


Figure 9. Transimpedance design with 2nd order passive postfilter

The input referred current noise is a low 0.4pA/√Hz through most of the span rising to 3.3pA/√Hz at 10MHz due to increasing N_G for the input voltage noise and the filter rolloff. Evaluating Equation 8 using a $\text{NPBW} = 11\text{MHz} \times 1.11 = 12.2\text{MHz}$ (the $F_{-3\text{dB}}$ to NPBW adjustment for a 2nd order Butterworth filter) gives an $i_{\text{eq}} = 2.2\text{pA}/\sqrt{\text{Hz}}$.

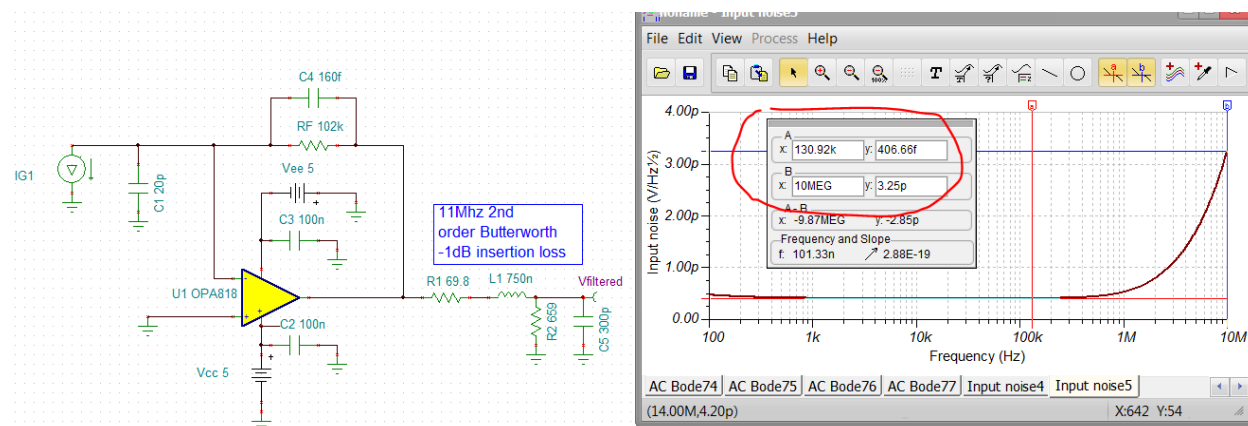


Figure 10. Input referred spot noise current referenced to filter output.

This design flow was simplified by assuming a closed loop Butterworth design target. Testing the LG phase margin in Figure 11 showed very nearly an exact (65.5deg) Butterworth phase margin.

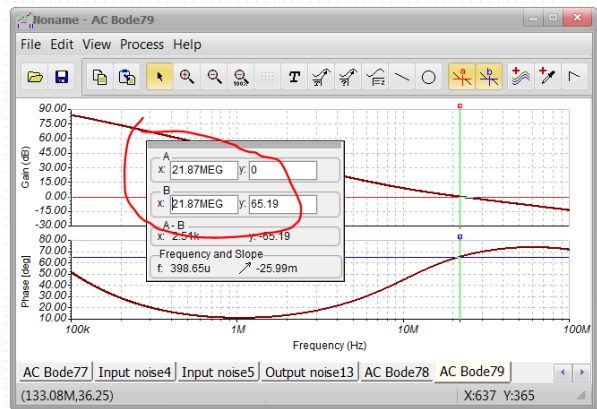
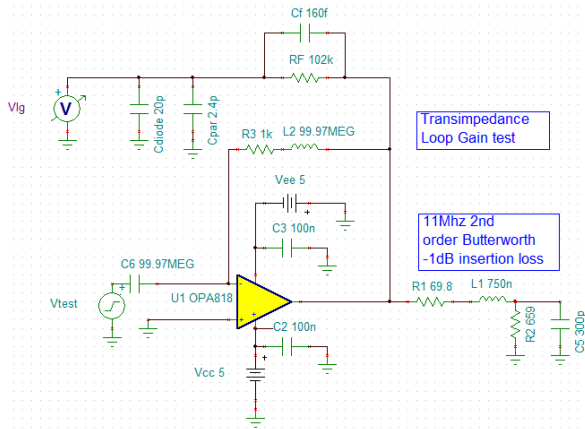


Figure 11. Transimpedance design Loop Gain phase margin

The nearly 180deg phase shift around the loop at lower frequencies is normal for transimpedance design as the NG zero (70kHz in this example) starts rising at lower frequencies. That loop phase is pulled back up to 65.2deg phase margin at LG=0dB crossover by the feedback pole. The high frequency noise gain is approximately $1 + (22.4\text{pf}/0.16\text{pF}) = 235\text{V/V}$. Such a high noise gain at higher frequencies shows why the higher order poles of a decompensated VFA can normally be ignored and only the true single pole GBP is required for the design.

Representative Decompensated VFA devices

The following 3 tables list a range of wideband decompensated voltage feedback amplifier solutions. Breaking these into technology segments as CMOS, JFET, and Bipolar inputs. The Bipolar will have the lowest input noise voltage's while the CMOS and JFET will have the lowest input noise current. Also, for the devices listed, an effort was made to extract the true single pole Gain Bandwidth Product to list in descending order. In some case that was a TINA simulation of the most current (circa June 2019) model where any capacitive load was removed for the A_{ol} simulation if noted in the specifications. That simulation result took precedence over other reported numbers or datasheet plots. In all cases, these are limited to –

- Single channel devices
- If both disable and non-disable versions, the disable version is shown.
- Not obsolete

Note that in many cases the reported Small Signal Bandwidth at G_{min} times that G_{min} value does not equal the true GBP.

Table 1. Decompensated CMOS Voltage Feedback Amplifiers.

		Sorted in Descending True GBP														
Supplier	Device	Operating total Vs (min V)	Operating total Vs (max V)	SSBW @ Gmin (MHz)	Gmin (V/V)	True GBP (MHz)	Slew Rate (V/μsec)	Icc Max/Ch (mA)	Vn_flatband (nV/√Hz)	Vos Max (mV)	Ib Max (nA)	Io (mA) (=min. linear)	R-R In	R-R Out	Output Headroom (V)	Part Description
NSM	LMP7717	1.8	5.5	8.8	10	109	24	1.4	5.8	0.150	1.00E-03	60	-Vs	Yes	0.080	88MHz Decompensated Precision, Low Noise Amp
Maxim	MAX44280	1.7	5.5	10.0	5	50	30	1.2	12.7	0.050	5.00E-04	40	Yes	Yes	0.100	1.8V, 50MHz, Low-Offset, Low-Power, Rail-to-Rail I/O Op Amp (AV-5)
Maxim	MAX40087	2.7	5.5	8.4	5	42	10	3.0	4.2	0.150	1.60E-01	20	-Vs	Yes	0.010	42MHz Low-Noise, Low Input Bias Single Op Amp in WLP and SOT23
ST Micro	TSV991A	2.5	5.5	5.0	4	21	10	1.1	27	1.5	1.00E-02	32	Yes	Yes	0.015	Wide bandwidth (20MHz) rail to rail input/output 5V CMOS Op-Amp, small Vos
Maxim	MAX4488	2.7	5.5	8.4	5	20	10	4.4	4.5	0.750	1.50E-01	24	-Vs	Yes	0.080	SOT23, Low-Noise/Distortion, Wideband, Rail-to-Rail Op Amp (AV-5)

This JFET table has the same screens as the CMOS table. Many more offerings here with much higher speed options over the CMOS devices. While the CMOS devices are usually CMOS implementations through the entire device, these are JFET “input” only with usually bipolar devices used everywhere else.

Table 2. Decompensated JFET Input voltage Feedback Amplifiers.

		Sorted in Descending True GBP														
Supplier	Device	Operating total Vs (min V)	Operating total Vs (max V)	SSBW @ Gmin (MHz)	Gmin (V/V)	True GBP (MHz)	Slew Rate (V/μsec)	Icc Max/Ch (mA)	Vn_flatband (nV/√Hz)	Vos Max (mV)	Ib Max (V+pin) nA	Io (mA) (=min. linear)	R-R In	R-R Out	Output Headroom (V)	Part Description
TI	OPA858	3.3	5.3	1200.0	7	5400	2000	24.0	2.5	5.000	5.00E-03	80	-Vs	No	0.900	5.5GHz Gain Bandwidth Product, Gain of 7V/V stable, FET Input Amplifier
LTC	LTC6268-10	3.1	5.3	400.0	10	3000	1000	18.0	4.0	0.700	9.00E-04	25	-Vs	Yes	0.090	Single 4GHz Ultra low bias current FET input op amp
TI	OPA818	6.0	13.0	790.0	7	2800	1400	29.0	2.2	1.250	2.00E-02	55	-Vs	No	1.200	2.7GHz, 13V, Gain of 7 Stable, JFET Input Op Amp
TI	OPA657	9.0	12.0	350.0	7	1600	700	16.0	4.8	1.800	2.00E-02	50	No	No	1.300	1.6GHz, Low Noise, Fet -Input Operational Amplifier
ADI	AD8067	5.0	24.0	75.0	6	280	640	7.0	6.6	1.000	5.00E-03	26	-Vs	Yes	0.150	High GBW Product, Rail-Rail Out, Precision FastFET™ Voltage Feedback Op Amp
ADI	ADA4637-1	8.0	36.0	29.0	5	79	170	7.5	4.8	0.300	5.00E-03	10	No	No	2.700	Single High Performance JFET Op Amp Decompensated (OPA637 cross)
TI	OPA637	9.0	36.0	16.0	5	76	135	7.5	4.5	0.100	5.00E-03	45	No	No	2.700	Precision High-Speed JFet Operational Amplifiers

The Bipolar devices have many more (and much older) alternatives. In order to eliminate devices perhaps not too interesting for new design, this table was also screened to only include -

1. Input offset voltage <=3.0mV
2. Input voltage noise <=3nV/√Hz

These are where the lowest input voltage noise and highest bandwidth devices will be found- but with much higher input bias currents and current noise terms.

Table 3. Decompensated Bipolar voltage feedback amplifiers.

		Sorted in Descending True GBP														
Supplier	Device	Operating total Vs (min V)	Operating total Vs (max V)	SSBW @ Gmin (MHz)	Gmin (V/V)	True GBP (MHz)	Slew Rate (V/μsec)	Icc Max/Ch (mA)	Vn_flatband (nV/√Hz)	Vos Max (mV)	Ib Max (V+pin) nA	Io (mA) (=min. linear)	R-R In	R-R Out	Output Headroom (V)	Part Description
TI	OPA855	3.3	5.3	2500.0	7	8000	2750	20.0	1.0	2.500	1.85E+04	80	No	No	0.900	8GHz Gain Bandwidth Product, gain of 7V/V Stable, Bipolar input amplifier
NSM	LMH6629	2.7	5.5	1000.0	10	3900	1600	16.7	0.7	0.780	2.30E+04	250	-Vs	No	0.900	Ultra low noise, High Speed Op Amp with Shutdown
ADI	AD8099	5.0	12.0	510.0	5	3800	470	16.0	1.0	0.500	1.30E+04	89	No	No	1.300	Ultralow Distortion, High Speed, Very Low Noise, Voltage Feedback Operational Amplifier
TI	OPA847	9.0	12.0	600.0	12	3000	950	18.4	0.9	0.500	3.90E+04	60	No	No	1.700	Wideband, Ultra-Low Noise, Voltage Feedback Operational Amplifier with Shutdown
TI	OPA846	9.0	12.0	500.0	7	1750	625	12.9	1.2	0.600	1.90E+04	65	No	No	1.700	Wideband, Low Noise, Voltage Feedback Operational Amplifier
NSM	LMH6624	5.0	12.0	95.0	20	1500	400	16.0	0.9	0.500	2.00E+04	100	No	No	1.100	Ultra Low Noise Wideband Operational Amplifier
ADI	ADA4895-1	3.0	10.0	236.0	10	1300	943	3.2	1.0	0.350	6.00E+03	80	-Vs	Yes	0.030	Low Power, InV/√Hz, G≥10 Stable, Rail-Rail Output Amplifier
LTC	LT6230-10	3.0	12.6	145.0	10	1300	320	3.9	1.1	0.500	1.00E+04	15	No	Yes	0.200	215MHz, Rail-to-Rail Output, 1.1nV/√Hz, 3.5mA Op Amp
TI	THS4021	9.0	32.0	350.0	10	1000	470	10.0	1.5	2.000	6.00E+03	80	No	No	2.500	350-MHz Ultra-Low Noise Voltage-Feedback Amplifier
TI	OPA843	9.0	12.0	500.0	3	800	1000	20.9	2.0	1.200	3.50E+04	90	No	No	2.000	Wideband, Low Distortion, Medium Gain, Voltage Feedback Operational Amplifier
LTC	LT1226	5.0	30.0	40.0	25	700	400	9.0	2.6	1.000	8.00E+03	19	No	No	1.700	Low Noise Very High Speed Operational Amplifier
LTC	LT1222	4.0	36.0	110.0	10	500	200	10.5	3.0	0.300	3.00E+02	20	No	No	2.000	500MHz, 3nV/√Hz, Av ≥ 10 Operational Amplifier
LTC	LT6233-10	3.0	12.6	37.5	10	320	115	1.4	1.9	0.500	3.00E+03	20	No	Yes	0.195	60MHz, Rail-to-Rail Output, 1.9nV/√Hz, 1.2mA Op Amp
TI	OPA838	2.7	5.4	90.0	6	300	350	1.0	1.8	0.125	2.80E+03	28	-Vs	Yes	0.100	1mA, 300MHz Gain Bandwidth, Voltage Feedback Op amp
TI	THS4031	9.0	32.0	100.0	2	116	100	10.0	1.6	2.000	8.00E+03	60	No	No	1.400	100-MHz Low Noise Voltage-Feedback Amplifier
ADI	AD797	10.0	36.0	8.0	10	105	20	10.5	0.9	0.080	1.50E+03	40	No	No	2.000	Ultralow distortion, Ultralow Noise op amp
LTC	LT1037	8.0	44.0	16.0	5	60	15	4.3	2.5	0.025	3.50E+01	21	No	No	1.500	Low Noise, High Speed Precision Op Amp (min gain 5V/V)
TI	OPA228	5.0	36.0	5.0	5	36	10	3.8	3.0	0.075	1.00E+01	45	No	No	2.000	High Precision, Low Noise Amplifier

The decompensated VFA finds wide application in simple higher gain applications where its intrinsically lower input voltage noise and higher slew rates are very useful. It is also very commonly used in transimpedance applications where their very high GBP expands the performance universe and the high NG at LG=0dB crossover renders a unity gain stability requirement unnecessary. Using the inverting compensation approach expands the application space to lower inverting gains and MFB filter applications. Next up – are inverting attenuators a stability risk and why might you use them?

References for Decompensated VFAs

1. TI OPA838 op amp, “1-mA, 300MHz, Voltage Feedback op amp”
<http://www.ti.com/lit/ds/symlink/opa838.pdf>
2. Planet Analog article “Stability Issues for High Speed Amplifiers: Introductory Background and Improved Analysis, Insight #5”, Michael Steffes, Feb. 3, 2019,
https://www.planetanalog.com/author.asp?section_id=3404&doc_id=565056&

3. Planet Analog article "Input Impedance Extraction and Application for High Speed Amplifiers, Insight #9", Michael Steffes, June 7, 2019, https://www.planetanalog.com/author.asp?section_id=3404&doc_id=565150
4. TI LMV793, "88MHz, Low Noise, CMOS Input, Decompensated Operational Amplifiers" (same as the LMP7717), <http://www.ti.com/lit/ds/symlink/lmv793.pdf>
5. EDN article "Unique compensation technique tames high bandwidth voltage feedback op amps", Michael Steffes, Feb. 27, 2019, <https://www.edn.com/design/analog/4461648/Unique-compensation-technique-tames-high-bandwidth-voltage-feedback-opamps>
6. TI OPA847 op amp, "Wideband, Ultra-Low Noise, Voltage Feedback Op Amp with Shutdown" <https://www.ti.com/lit/ds/symlink/opa847.pdf>
7. TI OPA818 op amp, "2.7GHz, 13V, decompensated 7V/V, FET input Op Amp" <http://www.ti.com/lit/ds/symlink/opa818.pdf>
8. TI application note, "Design Methodology for MFB Filters in ADC Interface Applications", Michael Steffes, Feb. 2006, <http://www.ti.com/lit/an/sboa114/sboa114.pdf>
9. Planet Analog article "Include the op amp gain bandwidth product in the Rauch low pass active filter performance equations", Michael Steffes, Feb. 8, 2018, https://www.planetanalog.com/author.asp?section_id=434&doc_id=564804
10. TI Active Filter Designer, entry page for filter type selection, <https://webench.ti.com/filter-design-tool/filter-response>
11. TI application note, "Transimpedance Considerations for High Speed Amplifiers", Xavier Ramus, Nov. 2009, <http://www.ti.com/lit/an/sboa122/sboa122.pdf>
12. TINA simulator available from DesignSoft for <\$350 for the Basic Plus edition. Includes a wide range of vendor op amps and is the standard platform for TI op amp models.
13. TI application note, "RLC Filter Design for ADC Interface Applications", Michael Steffes, Dec. 2003, <http://www.ti.com/lit/an/sbaa108a/sbaa108a.pdf>